A direct method to calculate thermal conductivity and its application in solid HMX

2010 J. Phys.: Condens. Matter 22 185404

(http://iopscience.iop.org/0953-8984/22/18/185404)

J. Phys.: Condens. Matter **22** (2010) 185404 (7pp) doi:10.1088/0953-8984/22/18/185404

A direct method to calculate thermal conductivity and its application in solid HMX

Y Long[1], J Chen[1], Y G Liu[2], F D Nie[2] and J S Sun[1]

[1] Laboratory of Computational Physics, Institute of Applied Physics and Computational Mathematics, PO Box 8009, Beijing 100088, People's Republic of China
[2] Institute of Chemical Materials, CAEP, Mianyang 621900, People's Republic of China

E-mail: long_yao@iapcm.ac.cn

Received 2 December 2009, in final form 30 March 2010
Published 15 April 2010
Online at stacks.iop.org/JPhysCM/22/185404

Abstract
The calculation of thermal conductivity for complex material systems is a challenging problem in computational materials science. Its key point is to calculate heat flux. In this work, we derive a concise formula for this purpose based on the equation of motion and then use it to study the thermal conduction properties of octahydro-1,3,5,7-tetranitro-1,3,5,7-tetrazocine (HMX), which is a widely used plastic-bonded explosive (PBX). The results are in fair agreement with experiments and show a distinct thermal conduction anisotropy for HMX single crystals. Then we investigate some key issues of thermal conductivity, such as its temperature-dependence and composition-dependence. A series of interesting results are obtained.

(Some figures in this article are in colour only in the electronic version)

1. Introduction

Thermal conductivity is an important performance factor for energetic materials. It affects the heat accumulation process in explosions and determines the explosive speed and pressure. The calculation of thermal conductivity is a challenging problem in explosives, as they usually have complex molecular structures. In this work, we use a self-derived heat flux formula to study this problem for octahydro-1,3,5,7-tetranitro-1,3,5,7-tetrazocine (HMX), which is a widely used plastic-bonded explosive (PBX) in industry and military engineering.

There are two ways to calculate thermal conductivity by molecular dynamics (MD), namely the direct and indirect methods. The former one is usually referred to as Müller-Plathe's work [1], and the latter one is the Green–Kubo formula [2–7]. For Plathe's method, the main idea is to set the heat flux (J) by interchanging high energy and low energy particles in a certain frequency, and then measuring the temperature gradient (∇T). Thermal conductivity is obtained by Fourier's law

$$\lambda = -\frac{J}{\nabla T}. \tag{1}$$

But in this work, we use another kind of direct method. The temperature field is preset and heat flux is calculated by a specific formula, different from Plathe's method.

The HMX we are interested in in this work is an important energetic material. It has high explosive speed, pressure, and energetic level, is the main component of many explosive products, such as PBX-9011, PBX-9404, PBX-9501 etc [8], so attracts much attention [9–15]. So far, a large number of experimental data have been accumulated, and theoretical analysis based on atomistic calculation is desired.

Furthermore, HMX is an organic material, consisting of C, N, O, and H, and has four crystalline phases α, β, γ, and δ. Among them, β is the most stable phase at low temperature (<380 K), and δ is the high temperature phase between 430 and 550 K, just below the melting point. These two typical phases are widely studied in many topics, such as thermal expansion, elastic constants and β–δ phase transformation, etc [13, 16–21]. Now we pay attention to their thermal conduction properties.

Figure 1 shows the atomic structures of β and δ-HMX. Their lattice constants are listed in table 1. We can see that β-HMX is a monoclinic crystal and δ-HMX is a hexagonal crystal. So for δ-HMX, the thermal conduction is equivalent in a and b directions. By the way, the HMX molecule is 'chair-like' in β phase and 'basket-like' in δ phase.

In summary, we will use a self-derived heat flux formula to study the thermal conduction properties of β and δ-HMX,

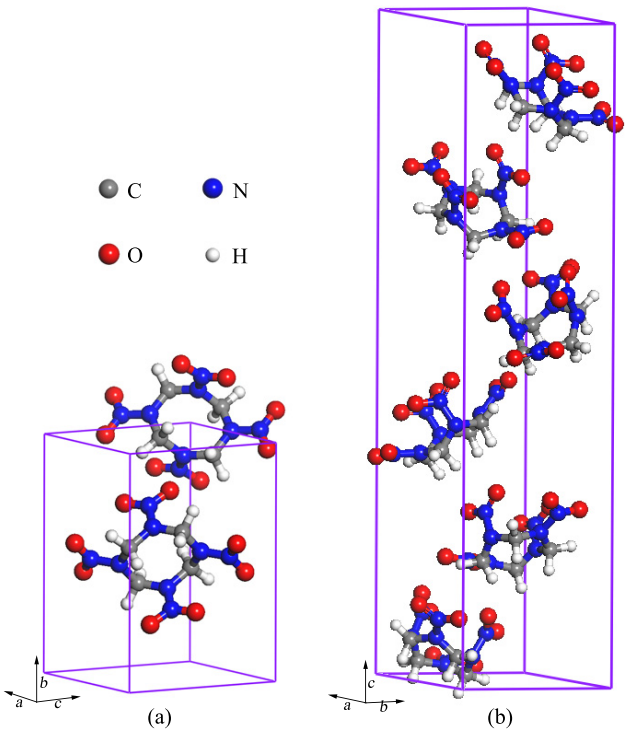

Figure 1. Atomic structures of (a) β and (b) δ-HMX.

Table 1. Lattice constants of β and δ-HMX, from [10, 11].

	a (Å)	b (Å)	c (Å)	α (deg)	β (deg)	γ (deg)
β-HMX	6.5347	11.0296	7.3549	90	102.69	90
δ-HMX	7.711	7.711	32.553	90	90	120

including thermal conductivity, thermal conduction anisotropy, temperature-dependence and composition-dependence, etc. A series of MD simulations will be performed, associated with careful post-treatment calculations. The following work consists of four parts. First, in section 2, we present the interatomic potentials used in this work. Then, in section 3, the method to calculate thermal conductivity is introduced, especially the heat flux formula. Next, in section 4, we perform MD simulations on β and δ-HMX. Their thermal conductivities are calculated and a series of relative properties are studied. Lastly, section 5 is the conclusion.

2. Interatomic potentials

In this work, we use quantum-based interatomic potentials for MD simulations. They were obtained by Smith and Bharadwaj in 1999 [22] and have been widely used in HMX calculations. Let us give a brief introduction below.

As we known, HMX is an organic material. Its atomic interactions include two parts:

$$V = V_{\text{Nonbond}} + V_{\text{Valence}} \tag{2}$$

where V is potential energy, V_{Nonbond} is nonbond interaction, and V_{Valence} is valence interaction.

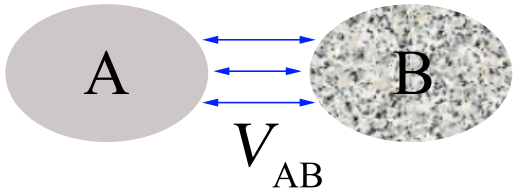

Figure 2. Two atom groups A and B contacted by a weak interaction V_{AB}.

For these two kinds of interactions, V_{Nonbond} is mainly intermolecular and V_{Valence} is just intramolecular. Both of them consist of several terms

$$\begin{aligned} V_{\text{Nonbond}} &= V_{\text{VDW}} + V_{\text{Coulomb}} \\ V_{\text{Valence}} &= V_{\text{Bond}} + V_{\text{Angle}} + V_{\text{Dihedral}} + V_{\text{Improper}} \end{aligned} \tag{3}$$

where V_{VDW} is the van der Waals interaction, V_{Coulomb} is the Coulomb interaction, V_{Bond} is bond energy, V_{Angle} is angle energy, V_{Dihedral} is dihedral energy and V_{Improper} is improper energy. The last two are four-body interactions. From this constitution, we see that V_{Nonbond} just includes pair potentials and V_{Valence} includes many-body potentials. A notable result is that intermolecular interactions are pair-bound.

Paying attention to their function forms, van der Waals energy is Buckingham style and valence energies are Harmonic style. They have a large number of potential parameters, as listed in table 2. In applications, these potentials have been used to study atomic structures, lattice constants, elastic constants, and thermal expansions of HMX [17–19, 22]. The results are in agreement with experiments, so it is reasonable to use them for thermal conductivity calculations now.

3. Methodology

In this section, we are going to introduce the method used in this work. It is a direct method. The key point is to calculate heat flux by a self-derived formula. For this purpose, let us consider two groups of atoms A and B, as shown in figure 2. The total energy is

$$U = E_{\text{A}} + V_{\text{A}} + E_{\text{B}} + V_{\text{B}} + V_{\text{AB}} \tag{4}$$

where U is total energy, E_{A} and E_{B} are kinetic energies of A and B, V_{A} and V_{B} are potential energies, and V_{AB} is the interaction energy between A and B.

Then, we use x_i ($i \in$ A or B) as atomic position, $\dot{x}_i$ as velocity, and $\ddot{x}_i$ as acceleration. For group A, the total energy is

$$U_{\text{A}} = E_{\text{A}} + V_{\text{A}} \tag{5}$$

kinetic energy is

$$E_{\text{A}} = \sum_{i \in \text{A}} \tfrac{1}{2} m_i \dot{x}_i^2, \tag{6}$$

and the equation of motion is

$$m_i \ddot{x}_i = -\frac{\partial V}{\partial x_i} = -\frac{\partial V_{\text{A}}}{\partial x_i} - \frac{\partial V_{\text{AB}}}{\partial x_i}, \qquad i \in \text{A} \tag{7}$$

where m_i is the mass of the ith atom.

Table 2. Potential parameters of HMX, from [18, 22].

Atom charge	
Atom type	q (electron)
C	−0.540 00
N (amine)	0.056 375
N (nitro)	0.860 625
O	−0.458 50
H	0.270 000

Van der Waals term, $V_{\mathrm{VDW}} = A\mathrm{e}^{-Br_{ij}} - \frac{C}{r_{ij}^6}$

Pair type	A (kcal mol^{-1})	B (Å^{-1})	C (kcal mol^{-1} Å^6)
C–C	14 976.0	3.090	640.8
C–N	30 183.57	3.435	566.03
C–O	33 702.4	3.576	505.6
C–H	4 320.0	3.415	138.2
N–N	60 833.9	3.780	500.0
N–O	67 925.95	3.921	446.6
N–H	12 695.88	3.760	116.96
O–O	75 844.8	4.063	398.9
O–H	14 175.97	3.901	104.46
H–H	2 649.7	3.740	27.4

Bond term, $V_{\mathrm{Bond}} = \frac{1}{2}K(r_{ij} - r_0)^2$

Bond type	K (kcal mol^{-1} Å^{-2})	r_0 (Å)
C–N	672.1	1.44
C–H	641.6	1.09
N–N	991.7	1.36
N–O	1990.1	1.23

Angle term, $V_{\mathrm{Angle}} = \frac{1}{2}K(\theta_{ijk} - \theta_0)^2$

Angle type	K (kcal mol^{-1} rad^{-2})	θ_0 (rad)
C–N–C	70.0	1.8430
C–N–N	130.0	1.6723
N–C–N	70.0	1.9289
N–C–H	86.4	1.8676
N–N–O	125.0	1.8754
O–N–O	125.0	2.1104
H–C–H	77.0	1.8938

Dihedral term, $V_{\mathrm{Dihedral}} = \frac{1}{2}K[1 - \cos(n\phi_{ijkl})]$

Dihedral type	K (kcal mol^{-1})	n
C–N–C–N	3.30	1
C–N–C–N	−1.61	2
C–N–C–N	0.11	3
C–N–C–H	−0.16	3
C–N–N–O	8.45	2
C–N–N–O	0.79	4
C–N–N–O	0.004	8

Improper term, $V_{\mathrm{Improper}} = \frac{1}{2}K\varphi_{ijkl}^2$

Improper type	K (kcal mol^{-1} rad^{-2})
C–N–C–*N	8.0
O–N–O–*N	89.3

If there are heat exchanges between A and B, the heat flux is

$$J_{\mathrm{A}\to\mathrm{B}} = -\frac{1}{S}\frac{\mathrm{d}U_{\mathrm{A}}}{\mathrm{d}t} = -\frac{1}{S}\frac{\mathrm{d}E_{\mathrm{A}}}{\mathrm{d}t} - \frac{1}{S}\frac{\mathrm{d}V_{\mathrm{A}}}{\mathrm{d}t}$$

$$= -\frac{1}{S}\sum_{i\in\mathrm{A}} m_i\dot{x}_i\ddot{x}_i - \frac{1}{S}\sum_{i\in\mathrm{A}}\dot{x}_i\frac{\partial V_{\mathrm{A}}}{\partial x_i}$$

$$= \frac{1}{S}\sum_{i\in\mathrm{A}}\dot{x}_i\left(\frac{\partial V_{\mathrm{A}}}{\partial x_i} + \frac{\partial V_{\mathrm{AB}}}{\partial x_i}\right) - \frac{1}{S}\sum_{i\in\mathrm{A}}\dot{x}_i\frac{\partial V_{\mathrm{A}}}{\partial x_i}$$

$$= \frac{1}{S}\sum_{i\in\mathrm{A}}\dot{x}_i\frac{\partial V_{\mathrm{AB}}}{\partial x_i} \tag{8}$$

where S is the contact area between A and B. Also, the heat flux from B to A is

$$J_{\mathrm{B}\to\mathrm{A}} = \frac{1}{S}\sum_{j\in\mathrm{B}}\dot{x}_j\frac{\partial V_{\mathrm{AB}}}{\partial x_j}. \tag{9}$$

Considering their time averages (denoted as $\langle\ \rangle$), we can prove that

$$\begin{aligned}\langle J_{\mathrm{A}\to\mathrm{B}}\rangle + \langle J_{\mathrm{B}\to\mathrm{A}}\rangle &= \frac{1}{S}\left\langle\sum_{i\in\mathrm{A}}\dot{x}_i\frac{\partial V_{\mathrm{AB}}}{\partial x_i} + \sum_{j\in\mathrm{B}}\dot{x}_j\frac{\partial V_{\mathrm{AB}}}{\partial x_i}\right\rangle \\ &= \frac{1}{S}\left\langle\frac{\mathrm{d}V_{\mathrm{AB}}}{\mathrm{d}t}\right\rangle \\ &= \frac{1}{S}\lim_{t\to\infty}\frac{V_{\mathrm{AB}}(t) - V_{\mathrm{AB}}(0)}{t} \\ &= 0.\end{aligned} \tag{10}$$

This shows that $J_{\mathrm{A}\to\mathrm{B}}$ and $J_{\mathrm{B}\to\mathrm{A}}$ are self-consistent.

Turning back to the HMX of interest in this work, we choose appropriate atom groups to make sure that no molecules are separated by different groups. As a result, just intermolecular interactions (pair-bound) are considered for heat flux calculations; valence energy terms are skipped. For convenience, let us denote the pair potential as $\varphi_{ij}(r_{ij})$, where $r_{ij} = |x_i - x_j|$ is the pair distance between atom i and j. In this way, V_{AB} is

$$V_{\mathrm{AB}} = \sum_{i\in\mathrm{A},\,j\in\mathrm{B}}\varphi_{ij}(r_{ij}). \tag{11}$$

Substituting it into (8), we get

$$\begin{aligned}J_{\mathrm{A}\to\mathrm{B}} &= \frac{1}{S}\sum_{i\in\mathrm{A},\,j\in\mathrm{B}}\dot{x}_i\frac{\partial\varphi_{ij}(r_{ij})}{\partial x_i} \\ &= \frac{1}{S}\sum_{i\in\mathrm{A},\,j\in\mathrm{B}}\dot{x}_i f_{ij}\end{aligned} \tag{12}$$

where $f_{ij} = \frac{\partial\varphi_{ij}(r_{ij})}{\partial x_i} = -f_{ji}$ is the force from i to j. Also, (9) can be rewritten as

$$J_{\mathrm{B}\to\mathrm{A}} = \frac{1}{S}\sum_{i\in\mathrm{A},\,j\in\mathrm{B}}\dot{x}_j f_{ji}. \tag{13}$$

As $\langle J_{\mathrm{A}\to\mathrm{B}}\rangle = -\langle J_{\mathrm{B}\to\mathrm{A}}\rangle$, an equivalent definition is obtained

$$\begin{aligned}J &= \tfrac{1}{2}(J_{\mathrm{A}\to\mathrm{B}} - J_{\mathrm{B}\to\mathrm{A}}) \\ &= \frac{1}{2S}\sum_{i\in\mathrm{A},\,j\in\mathrm{B}}(\dot{x}_i f_{ij} - \dot{x}_j f_{ji}) \\ &= \frac{1}{2S}\sum_{i\in\mathrm{A},\,j\in\mathrm{B}}(\dot{x}_i + \dot{x}_j)f_{ij},\end{aligned} \tag{14}$$

which satisfies $\langle J\rangle = \langle J_{\mathrm{A}\to\mathrm{B}}\rangle = -\langle J_{\mathrm{B}\to\mathrm{A}}\rangle$.

Equation (14) is the final heat flux formula used in this work. It is derived from the basic equation of motion, and

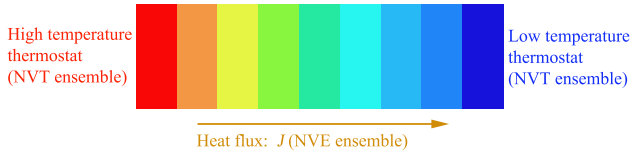

Figure 3. The layer-by-layer model for thermal conductivity calculation.

expresses heat flux by atomic velocities and forces, so can be applied in MD. Comparing this with the one derived for the Green–Kubo method [23], this derivation is very concise and also reasonable. It has an advantage that valence energy terms are excluded by choosing appropriate atom groups. However, there is also a limitation of this formula. It demands that the atoms in group A and B be non-swappable, so can only be applied in solid materials, not liquids.

In order to calculate thermal conductivity, we build a layer-by-layer model, as shown in figure 3. Each layer is treated as one atom group mentioned above. In MD simulation, the left and right layers are NVT ensembles, in high and low temperatures respectively. The middle layers are NVE ensembles, whose equation of motion is (7). Heat flux can be calculated by (14) and temperature gradient is measured directly. Resultant thermal conductivity is obtained by (1).

NVE means 'constant particle number, volume, and energy'. It is the simplest ensemble and just follows the basic equation of motion (see (7)). NVT means 'constant particle number, volume, and temperature'; it asks for a thermostat algorithm to keep temperature. In this work, we use a Nose–Hoover thermostat [24, 25] for the NVT ensemble.

4. Results

Now we are in a position to perform MD simulations and calculate thermal conductivity by simulated results. The MD program used in this work is LAMMPS [26], the time step is 0.5 fs, and the number of simulated steps is 10 000 (=5 ps).

Figure 4 shows a simulation model of δ-HMX. It has 6000 atoms, 6000 bonds, 10 000 angles, 9000 dihedrals, and 2000 impropers, according to the energy types in table 2. As Coulomb interaction and valence energy terms consume many computational resources, we choose middle size models to study. In this work, 16 CPUs are used for parallel computing, consuming 3 h for the model in figure 4.

The simulated temperature range is 430–550 K for δ-HMX (marked in figure 4) and 50–380 K for β-HMX. These wide ranges are chosen because HMX has a very small thermal conductivity. We need to set a large temperature gradient (or wide temperature range) to make sure that heat flux is distinct from possible fluctuation errors.

Furthermore, the specific direction of target of thermal conductivity is along the expected heat flux's direction, which is vertical to the layers illustrated in figure 3. For illustration, the model in figure 4 is used to calculate λ_a of δ-HMX. A series of similar models are constructed for other calculations.

By the way, thermal conductivities have been calculated for some small models (just about 1000 atoms) for testing. By using the time average and space average methods mentioned below, the results are not sensitive to model size. So we choose middle size models for the following calculations. They have fewer than 10 000 atoms.

Table 3 shows the calculated results of β and δ-HMX, where λ_a, λ_b, and λ_c are thermal conductivities in a, b, and c directions, and $\bar{\lambda}$ is the average value. Also, the available results from others' works are presented in the same table for comparison. Due to the symmetry of the hexagonal crystal, λ_a is equal to λ_b for δ-HMX.

From these results, an HMX single crystal has a non-negligible thermal conduction anisotropy. Its thermal conductivity is changed by about 20% in a, b, and c directions. The average value $\bar{\lambda}$ is for polycrystalline systems. It is worth noting that $\bar{\lambda}$ is in fair agreement with experiment and other calculations (in melting state), just a little higher. This is because we study perfect crystals in this work, the possible defects in actual materials are ignored. In principle, defects can disperse heat flux, so decrease thermal conduction efficiency, resulting in a reduction of thermal conductivity. This is why theoretical values are higher than experimental results.

In our mind, the function of defects in thermal conduction can also be studied by this heat flux formula. But it asks for complex model construction and theoretical analysis, so needs preparation. This work concentrates on the method and single crystals. Advanced studies of defects will be the subject of future work.

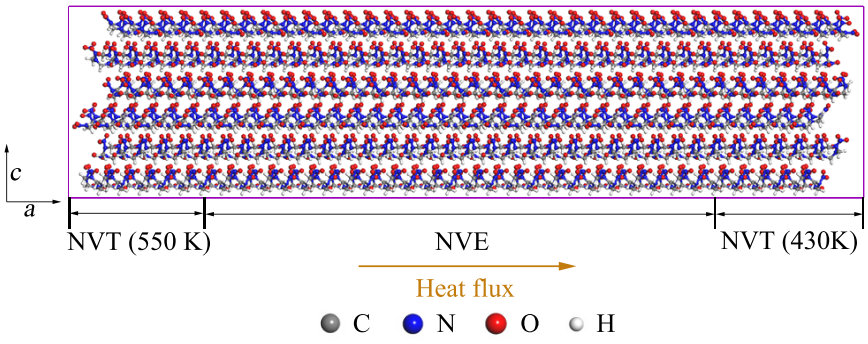

Figure 4. A simulation model of δ-HMX. The temperature is from 550 K (left) to 430 K (right).

Table 3. Thermal conductivities of HMX by calculations and experiments (W m^{-1} K^{-1}).

	This work				Bedrov[a]	Parr[b]	LASL[c]	Dong[d]
	λ_a	λ_b	λ_c	$\bar{\lambda}$	Calc.	Expt.	Expt.	Expt.
β-HMX	0.4718	0.8008	0.6618	0.6448	0.39	0.44	0.42	0.29
δ-HMX	0.3961	0.3961	0.5295	0.4406				

[a] For fluid HMX above 550 K [27]. [b] Reference [12]. [c] Reference [8]. [d] Reference [28].

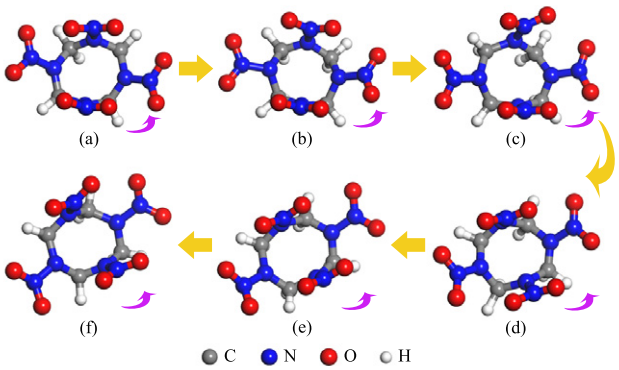

Figure 5. A rotating molecule in δ-HMX, extracted from MD simulated results. The time points are (a) 0 ps, (b) 0.4 ps, (c) 0.8 ps, (d) 1.2 ps, (e) 1.6 ps, and (f) 2 ps.

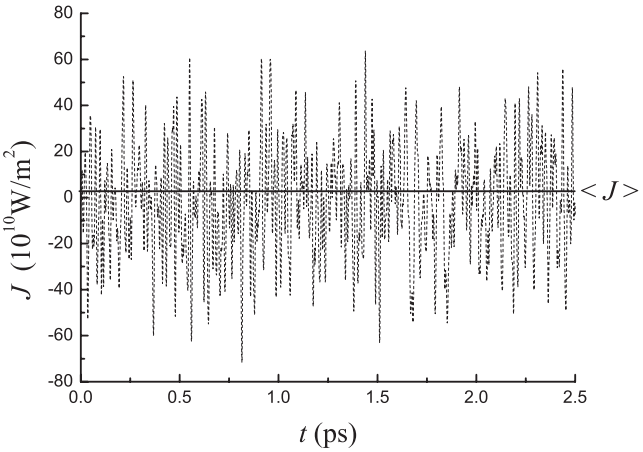

Figure 6. Heat flux fluctuation of β-HMX at 300 K, in a small area of 200 Å^2. The solid line denotes the expected $\langle J \rangle$ value.

Moreover, table 3 does not present experimental data for anisotropic thermal conductivities. This is related to the synthesis technology of HMX [29]. In fact, the available HMX single crystal is very small, just hundreds of microns. Its anisotropic thermal conductivities are hard to measure. So we just present the available isotropic data in table 3. The calculation of anisotropic properties in this work is a valuable evaluation.

And then, we study some key issues of thermal conductivity. The first is molecular rotation. From simulated results, we see that HMX molecules are rotating at 430–550 K, in δ phase, as shown in figure 5. Equation (14) demonstrates that this rotation also contributes to heat flux. So for HMX, the constitution of thermal conductivity is complex and includes contributions from atomic oscillation (or phonon) and molecular rotation. Fortunately, our method is based on the equation of motion. It can work well whether the molecules are rotating or not.

By detailed analysis of this rotation, we find out a temperature-dependence mechanism for thermal conductivity. It follows the path of 'temperature increase' → 'molecular rotation' → 'phonon dispersion' → 'phonon lifetime reduction' → 'thermal conductivity decrease'. For a discussion, molecules tend to rotate at high temperature. The rotating molecules can disperse phonons, so reduce phonon lifetime. Due to the thermal conduction-phonon theory [30–32], thermal conductivity is approximately proportional to this lifetime. Short phonon lifetime makes low thermal conductivity. As a result, for HMX, high temperature leads to low thermal conductivity. This is consistent with the calculated results, as shown in table 3. The thermal conductivity of δ-HMX (high temperature phase) is smaller than that of β-HMX (low temperature phase).

The second key issue is about heat flux fluctuation. This is a notable problem in calculations, as thermal fluctuation is distinct at the nanoscale. For illustration, figure 6 shows the instant heat flux (J) in β-HMX at 300 K, extracted from simulated results. The solid line denotes the expected time average value $\langle J \rangle$. In fact, the amplitude of J is several times larger than $\langle J \rangle$. So we need to make efforts to reduce possible fluctuation errors. Two methods are applied, by time average and space average, respectively. In the timescale, 10 000 simulation steps are performed in MD and the last 5000 steps' data are used for thermal conductivity calculations. In the space scale, a series of $\langle J \rangle$ at different positions on heat flux path are calculated for an average. By using these two methods, fluctuation is under control. Resultant thermal conductivities are presented in table 3.

The third issue is about the composition-dependence of thermal conductivity. In order to study this problem, two kinds of partial heat fluxes are defined. The first is for atom pairs, the pair flux, and the second is for single components, the atom flux.

From (14), heat flux is contributed by atom pairs. As HMX has four components C, N, O, and H, there are 10 kinds of pairs C–C, C–N, C–O, C–H, etc. We can decompose the total heat flux into 10 pair fluxes. For example, $J_{\mathrm{C-N}}$ is defined as

$$J_{\mathrm{C-N}} = \frac{1}{2S} \sum_{\substack{i\in \mathrm{A},\, j\in \mathrm{B} \\ (i,j)=\mathrm{C-N\ or\ N-C}}} (\dot{x}_i + \dot{x}_j) f_{ij}. \qquad (15)$$

The statement '$(i, j) =$ C–N or N–C' means the element type of the (i, j) pair is C–N or N–C. Other pair fluxes are defined

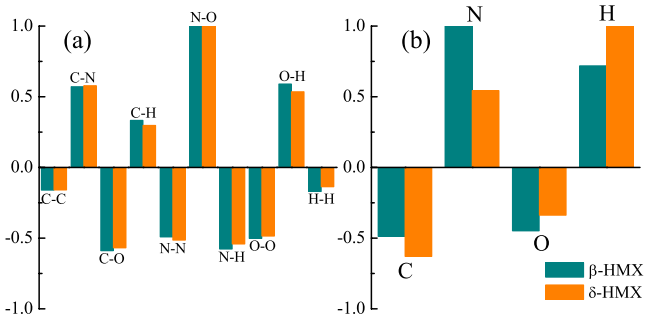

Figure 7. Normalized partial flux distributions for β and δ-HMX. (a) Pair fluxes, (b) atom fluxes: (b) is derived from (a).

in the same way. They satisfy

$$J = J_{\mathrm{C-C}} + J_{\mathrm{C-N}} + J_{\mathrm{C-O}} + J_{\mathrm{C-H}} + \cdots + J_{\mathrm{H-H}}. \quad (16)$$

Figure 7(a) displays the calculated pair flux distributions for β and δ-HMX. The results are normalized by setting the largest value as 1. From the figure, β and δ-HMX have a similar distribution. The pair flux is largest for N–O and smallest for C–C and H–H.

Based on pair fluxes, we can study atom fluxes for single components. They are defined as

$$\begin{aligned} J_{\mathrm{C}} &= J_{\mathrm{C-C}} + \tfrac{1}{2}J_{\mathrm{C-N}} + \tfrac{1}{2}J_{\mathrm{C-O}} + \tfrac{1}{2}J_{\mathrm{C-H}} \\ J_{\mathrm{N}} &= \tfrac{1}{2}J_{\mathrm{C-N}} + J_{\mathrm{N-N}} + \tfrac{1}{2}J_{\mathrm{N-O}} + \tfrac{1}{2}J_{\mathrm{N-H}} \\ J_{\mathrm{O}} &= \tfrac{1}{2}J_{\mathrm{C-O}} + \tfrac{1}{2}J_{\mathrm{N-O}} + J_{\mathrm{O-O}} + \tfrac{1}{2}J_{\mathrm{O-H}} \\ J_{\mathrm{H}} &= \tfrac{1}{2}J_{\mathrm{C-H}} + \tfrac{1}{2}J_{\mathrm{N-H}} + \tfrac{1}{2}J_{\mathrm{O-H}} + J_{\mathrm{H-H}}. \end{aligned} \quad (17)$$

It is obvious that

$$J = J_{\mathrm{C}} + J_{\mathrm{N}} + J_{\mathrm{O}} + J_{\mathrm{H}}. \quad (18)$$

Figure 7(b) shows the calculated results, also normalized.

For a discussion, J_{C}, J_{N}, J_{O}, and J_{H} denote the contributions of C, N, O, and H to heat flux in HMX. As thermal conductivity is proportional to heat flux (see (1)), figure 7 also denotes the thermal conductivity distributions.

From the figure, N and H contribute positively to thermal conductivity, C and O contribute negatively to it. This is different from pair flux distribution, in which the N–O pair contributes most, C–C and H–H contribute least. As a result, N and H components tend to increase the thermal conductivity of HMX, C and H tend to decrease it. For explosives, high thermal conductivity leads to low sensitivity. So N-rich and H-rich additives are beneficial for HMX's desensitizing.

At last, we turn back to methodology again. The direct method used in this work is different from the one introduced by Müller-Plathe [1]. Its key issue is a self-derived heat flux formula. This method has some features. First is that many-body valence energies can be excluded by choosing appropriate atom groups in applications. This can greatly simplify calculations. Second is that the heat flux formula is derived from the equation of motion directly. It is applicable from low temperature to high temperature, no matter whether the molecules are rotating or not. Third is that heat flux can be decomposed into pair fluxes and atom fluxes by this formula. Composition-dependence of thermal conductivity is studied. As well as these advantages, this method also has a limitation. It requires a non-diffusion system, so cannot be applied to the liquid state. Some improvements are expected in future work.

5. Conclusion

In this work, we derive a heat flux formula from the basic equation of motion and then use it to study the thermal conduction properties of β and δ-HMX. Some interesting results are obtained.

First, thermal conductivities are calculated. The results are in fair agreement with experiments, just a little higher. And thermal conduction anisotropy is evaluated for HMX single crystals, in an amplitude of 20%.

Then, we find out a possible temperature-dependence mechanism for thermal conductivity. It follows the path 'temperature increase' → 'molecular rotation' → 'phonon dispersion' → 'phonon lifetime reduction' → 'thermal conductivity decrease'. As a result, high temperature leads to low thermal conductivity. This is inconsistent with calculated results.

Next, heat flux fluctuation is investigated; it is notable in nanoscale calculations. Time average and space average methods are used to control this fluctuation.

Lastly, the composition-dependence of thermal conductivity is studied. We find that for HMX, N and H contribute positively to thermal conductivity, but C and O contribute negatively to it. This means that N-rich and H-rich additives are beneficial for HMX's desensitizing.

Acknowledgments

The authors gratefully acknowledge Professor D Q Wei and Dr S Liu for supporting the HMX models. This work is supported by the 973 project in China (No 61383), Foundation of National Key Laboratory (No 9140C6904020807) and National Natural Science Foundation of China (No 1077401).

References

[1] Müller-Plathe F 1997 A simple nonequilibrium molecular dynamics method for calculating the thermal conductivity *J. Chem. Phys.* **106** 6082
[2] Kubo R, Toda M and Hashitsume N 1997 *Statistical Physics II: Nonequilibrium Statistical Mechanics* (Berlin: Springer)
[3] Vogelsang R, Ciccotti G and Hoheisel C 1987 Thermal conductivity of the Lennard-Jones liquid by molecular dynamics calculations *J. Chem. Phys.* **86** 6371
[4] Lindan P J D and Gillan M J 1991 A molecular-dynamics study of the thermal-conductivity of CaF_2 and UO_2 *J. Phys.: Condens. Matter* **3** 3929
[5] Heyes D M 1994 Transport-coefficients of simple fluids with steeply repulsive potentials *J. Phys.: Condens. Matter* **6** 6409
[6] Sharma R K, Tankeshwar K and Pathak K N 1995 Transport-coefficients of classical dense fluids—a simple approach *J. Phys.: Condens. Matter* **7** 537
[7] Schelling P K, Phillpot S R and Keblinski P 2002 Comparison of atomic-level simulation methods for computing thermal conductivity *Phys. Rev.* B **65** 144306

[8] Gibbs T R and Popolato A (ed) 1980 *LASL Explosive Property Data* (California: University of California Press)
[9] Cady H H, Larson A C and Cromer D T 1963 The crystal structure of α-HMX and a refinement of the structure of β-HMX* *Acta Crystallogr.* **16** 617
[10] Choi C S and Boutin H P 1970 A study of the crystal-structure of β-crclotetramethylene tetranitramine by neutron diffraction *Acta Crystallogr.* B **26** 1235
[11] Cobbledick R E and Small R W H 1974 The crystal structure of the δ-form of 1,3,5,7-tetranitro-1,3,5,7-tetraazacyclooctane (δ-HMX) *Acta Crystallogr.* B **30** 1918
[12] Hanson-Parr D M and Parr T P 1999 Thermal properties measurements of solid rocket propellant oxidizers and binder materials as a function of temperature *J. Energetic. Mater.* **17** 1
[13] Weese R K, Maienschein J L and Perrino C T 2003 Kinetics of the $\beta \rightarrow \delta$ solid–solid phase transition of HMX, octahydro-1,3,5,7-tetranitro-1,3,5,7-tetrazocine *Thermochim. Acta* **401** 1
[14] Stevens L L and Eckhardt C J 2005 The elastic constants and related properties of β-HMX determined by Brillouin scattering *J. Chem. Phys.* **122** 174701
[15] Yoh J J-I 2006 Analysis of phase front structures for energetic materials *J. Phys.: Condens. Matter* **18** 8179
[16] Henson B F, Asay B W, Sander R K, Son S F, Robinson J M and Dickson P M 1999 Dynamic measurement of the HMX $\beta \rightarrow \delta$ phase transition by second harmonic generation *Phys. Rev. Lett.* **82** 1213
[17] Bedrov D, Smith G D and Sewell T D 2000 Temperature-dependent shear viscosity coefficient of octahydro-1,3,5,7-tetranitro-1,3,5,7-tetrazocine (HMX): a molecular dynamics simulation study *J. Chem. Phys.* **112** 7203
[18] Bedrov D, Arragari C, Smith G D, Sewell T D, Menikoff R and Zaug J M 2001 Molecular dynamics simulations of HMX crystal polymorphs using a flexible molecule force field *J. Comput.-Aided Mater. Des.* **8** 77
[19] Sewell T D, Menikoff R, Bedrow D and Smith G D 2003 A molecular dynamics simulation study of elastic properties of HMX *J. Chem. Phys.* **119** 7417
[20] Lu L-Y, Wei D-Q, Chen X-R, Lian D, Ji G-F, Zhang Q-M and Gong Z-Z 2008 The first principle studies of the structural and vibrational properties of solid β-HMX under compression *Mol. Phys.* **106** 2569
[21] Lian D, Lu L-Y, Wei D-Q, Zhang Q-M, Gong Z-Z and Guo Y-X 2008 High-pressure behaviour of β-HMX crystal studied by DFT-LDA *Chin. Phys. Lett.* **25** 899
[22] Smith G D and Bharadwaj R K 1999 Quantum chemistry based force field for simulations of HMX *J. Phys. Chem.* B **103** 3570
[23] Irving J H and Kirkwood J G 1950 The statistical mechanical theory of transport processes. IV. The equations of hydrodynamics *J. Chem. Phys.* **18** 817
[24] Nose S 1984 A molecular dynamics method for simulations in the canonical ensemble *Mol. Phys.* **52** 255
[25] Hoover W G 1985 Canonical dynamics: equilibrium phase-space distributions *Phys. Rev.* A **31** 1695
[26] Plimpton S J 1995 Fast parallel algorithms for short-range molecular dynamics *J. Comput. Phys.* **117** 1 http://lammps.sandia.gov.
[27] Bedrov D, Smith G D and Sewell T D 2000 Thermal conductivity of liquid octahydro-1,3,5,7-tetranitro-1,3,5,7-tetrazocine (HMX) from molecular dynamics simulations *Chem. Phys. Lett.* **324** 64
[28] Dong H S, Hu R Z, Yao P and Zhang X Y 2002 *ThermoGRAMS of Energetic Materials* (Beijing: National Defense Industry Press)
[29] Wei X W 2006 HMX re-crystallization and characterization *Masters Thesis* SiChuan University
[30] Ladd A J C, Moran B and Hoover W G 1986 Lattice thermal conductivity: a comparison of molecular dynamics and anharmonic lattice dynamics *Phys. Rev.* B **34** 5058
[31] Klements P G 1958 *Solid State Physics* vol 7 (New York: Academic)
[32] Peierls R E 1929 Kinetic theory of heat conduction in crystals *Ann. Phys.* **3** 1055